Taylor & Francis
Taylor & Francis Group

Particulate Science and Technology

An International Journal

ISSN: 0272-6351 (Print) 1548-0046 (Online) Journal homepage: http://www.tandfonline.com/loi/upst20

Magnetite Nanoparticles as Adsorbent Material for Cu^{2+} Ions from Aqueous Solution

Erlen Yizenia Cruz Jorge, Ricardo Martínez Sánchez, Juan Jiménez Chacón, Sergio Díaz Castañón & Francisco Calderón Piñar

To cite this article: Erlen Yizenia Cruz Jorge, Ricardo Martínez Sánchez, Juan Jiménez Chacón, Sergio Díaz Castañón & Francisco Calderón Piñar (2017): Magnetite Nanoparticles as Adsorbent Material for Cu^{2+} Ions from Aqueous Solution, Particulate Science and Technology, DOI: 10.1080/02726351.2017.1305028

To link to this article: http://dx.doi.org/10.1080/02726351.2017.1305028

Accepted author version posted online: 20 Mar 2017.

Magnetite Nanoparticles as Adsorbent Material for Cu^{2+} Ions from Aqueous Solution

Erlen Yizenia Cruz Jorge

Institute of Material Science and Technology, University of Havana, Havana, Cuba

Ricardo Martínez Sánchez*

Institute of Material Science and Technology, University of Havana, Havana, Cuba

Juan Jiménez Chacón

Institute of Material Science and Technology, University of Havana, Havana, Cuba

Sergio Díaz Castañón

Advanced Materials Division, IPICYT, San Luis Potosí, México

Francisco Calderón Piñar

Institute of Material Science and Technology, University of Havana, Havana, Cuba

CINVESTAV- Querétaro Unit, IPN, Queretaro, México

***Address correspondence to Ricardo Martínez Sánchez. E-mail:**

ricardo@imre.uh.cu

Abstract

Cu^{2+} ions can cause serious injuries to human health, at both high and low concentrations. Therefore, it is important not only to remove Cu^{2+} ions from aqueous media, but also to develop analytical methods for their accurate determination at low concentrations. Magnetite is one of the

most used sorbents for Cu^{2+} removal. This work aims at synthesizing magnetite nanoparticles and at evaluating their adsorption capacity toward Cu^{2+} ions in aqueous solution by means of atomic absorption spectroscopy. Magnetite nanoparticles were characterized by means of vibrational magnetometer, FTIR, XRD and TGA. Magnetic nanoparticles showed Ms values of 52 and 62 emu/g. By taking into consideration the precipitation of $Cu(OH)_2$ as a function of pH in the evaluation of the adsorption capacity of magnetite, we found that the maximum Cu^{2+} adsorption occurs at pH = 7 and that the adsorption equilibrium of the two samples is reached at 490 and 445 min. The use of blank solution avoids the overestimation of the adsorption capacity due to the presence of insoluble $Cu(OH)_2$. Finally, two models are considered as a liquid/solid phase reaction, pseudo-first and pseudo-second order reaction. Batch adsorption kinetics agrees with a pseudo-second order model suggesting that chemisorption is the rate-limiting step.

Keywords:

INTRODUCTION

Heavy metals contamination of water has become a major environmental problem due to fast industrialization and rising worldwide population. Unlike organic contaminants, which are susceptible to biological degradation, metallic ions do not become in easily innocuous final products since they are not biodegradable and tend to accumulate in living organisms. In addition, much of them are known to be highly toxic or carcinogenic (Fu and Wang 2011), e.g. Cr^{4+}, Hg^{2+}, Ni^{2+}, Zn^{2+}, Cd^{2+} and Cu^{2+}. In particular, excess of Cu^{2+} ions in human can provoke vomits, cramps, convulsions (Fu and Wang 2011), insomnia and liver damages.(Davidson 2010) On the contrary, deficiency of Cu^{2+} ions is related to other pathologies: anemia, neutropenia and osseous demineralization (Soltero-Baeza et al. 2007). Hence, it is important not only to remove

Cu^{2+} ions from aqueous media, but also to develop analytical methods for their accurate determination at low concentrations.

There are several strategies for water treatment seeking to eliminate heavy metal ions. They include chemical precipitation (Roy and Bhattacharya 2012), ionic exchange (Karami 2013), electrolysis (Fu), inverse osmosis and adsorption techniques (Farrukh et al. 2013). The choice depends on the cost, complexity and efficacy. Adsorption methods are economic, efficient and promissory. Iron oxides are included among the adsorbents used to remove heavy metals from residual waters (Teja and Koh 2009). Magnetite (Fe_3O_4) is the most important member of this family (Jiuhui 2008); it has been largely employed as sorbent for removing ionic species (Hg^{2+}, Cd^{2+}, Cr^{4+}, Cu^{2+} and Pb^{2+}) (Katsumata et al. 2003), organic contaminants and biological materials from water (Cotten, Navratil, and Eldredge 1999). The reasons for the wide use of magnetite as sorbent material relies on its low cost, its simple and fast synthesis (Gong et al. 2009), the treatment of large volumes of water (Roy and Bhattacharya 2012) as well as due to the possibilities of extraction of magnetite from the adsorption medium by applying an external magnetic field. Moreover, Fe_3O_4 can be prepared as nanoparticles; a structure by which the surface area is largely increased and subsequently, the amounts of the adsorbed contaminants can also be increased (Liu et al. 2009).

The removal of heavy metallic ions with Fe_3O_4 occurs by a process of chemical adsorption (Ortiz 2000; Navratil and Akin 2009). Depending on the metal type and the solution pH, many metallic ions form insoluble hydroxides. OH^- ions are strongly adsorbed on the surface of Fe_3O_4 particles acting as active centers for the adsorption of metallic ions (Navratil and Akin 2009). When magnetic Fe_3O_4 nanoparticles are used, diffusion of metallic ions from

solution to the active centers is favored (Karami 2013) thus providing a high capacity of adsorption (Giraldo, Erto, and Pirajan 2013).

Previous works are devoted to the utilization of magnetite for the removal of Cu^{2+} from water (Predescu et al. 2012; Giraldo, Erto, and Pirajan 2013; Karami 2013). In these studies, quantification of Cu^{2+} is usually accomplished from its content in solution but without taking into consideration the possible formation of $Cu(OH)_2$ at the pH of solution. In the present work, we report a detailed study on the adsorption behavior of magnetite nanoparticles toward Cu^{2+} ions. With this aim, we synthesized magnetite nanoparticles, evaluated their magnetic properties and performed their structural characterization. We particularly focused on the influence of the solution pH and the contact time between sorbent and ions on the adsorption capacity of magnetite nanoparticles, where the precipitation of $Cu(OH)_2$ as a function of pH was taken into consideration in the evaluation of the adsorption capacity of the adsorbent.

EXPERIMENTAL

Materials

Analytical grade reagents were used: $FeCl_2{\cdot}4H_2O$, 99% and $FeCl_3$ anhydrous, 97% (Sigma–Aldrich); NaOH, 99%, HNO_3, 65%, HCl, 37% and acetone, 99.5% (Panreac); $HClO_4$, 60% and formic acid, 98% (Merck); $NaNO_3$, 99.8%, $NaHPO_3$, 99.5% (Reachim); Na_2HPO_3, 99.5% (Riedel de Haën). Cu^{2+} solutions were prepared from $Cu(NO_3)_2$ standard solution of 1000 mg/L (Uni-Chem).

Synthesis of Magnetite

Magnetite was obtained by controlled co-precipitation (Massart 1981) of $FeCl_2$ and $FeCl_3$ salts in NaOH solution. 50 ml of $FeCl_2$ 1 mol/L and $FeCl_3$ 2 mol/L solutions in HCl 2 mol/L were first prepared. 4 ml of Fe^{2+} and 16 ml of Fe^{3+} solutions were mixed and dropped over 250 ml of NaOH 1.5 mol/L under magnetic stirring (Heidolph type MR Hei-Standard) at 1500 rpm and under N_2 atmosphere. The resulting black precipitate was separated using an external magnet. NaOH excess was neutralized with a solution of $HClO_4$ 0.5 mol/L. The solid was washed successively with water (to pH = 7) and acetone and vacuum-dried. Samples M1 and M2 were obtained by the same procedure.

Influence of pH and Interaction Time in the Removal of Cu^{2+} from Solution

Determination of the pH of Maximum Adsorption

Six blank solutions (P) and six working solutions (M_i), with pH values of 2, 4, 6, 7, 8 and 9 were prepared. pH values were adjusted with buffers: Na_2HPO_3 for pH ≥ 7 and formic acid for pH < 7. In all the solutions the concentration of $Cu(NO_3)_2$ and $NaNO_3$ (as regulator of the ionic strength) were set at 5 mg/L and 0.1 mol/L, respectively. Working dispersions were prepared by adding 0.01 g of magnetite sample to 20 ml of M_i solutions. Then, P and M_i solutions were shaken in a vibrating shaker (HDL APPARATUS HZS-H) at 120 rpm and 30°C for 24 hours. After this time, magnetite nanoparticles were magnetically separated from the dispersions. Subsequently, P and M_i solutions were filtered with 0.42 μm filters to remove the precipitate of $Cu(OH)_2$. Finally, the amounts of Cu^{2+} ions remaining in solution were determined by AAS. This procedure was performed three times for each magnetite sample.

Determination of the Time of Maximum Adsorption

250 ml of solution of 10 mg/L $Cu(NO_3)_2$ and 0.1 mol/L $NaNO_3$ were prepared. The pH of the solution was adjusted to 7 with $NaHPO_4$. The solution was left for 1 hour and then filtered with 0.42 μm filters to remove the $Cu(OH)_2$ precipitate. 200 ml of the filtrate were collected. 4 mL were used as a blank solution and the remaining 196 mL were mixed with 0.02 g of Fe_3O and stirred in a vibrating shaker at 120 rpm at 30°C. Aliquots of 4 ml were taken at different time intervals and the concentration of Cu^{2+} ion was determined by AAS. This procedure was performed three times for each sample of magnetite.

Material Characterization

FTIR spectra were recorded in a JASCO 4100 spectrometer in transmission mode by using standard KBr pellet technique. X-ray diffraction (XRD) measurements were performed in a Rigaku Dmax 2100 difractometer, (Co Kα = 0.17902 nm, 30 kV, 20 mA, step size of 0.02º). The mean particle size, τ, which may be smaller or equal to the particle size, were obtained by means of the Scherrer equation: (Chen et al. 2011)

$$\tau = \frac{K\lambda}{\beta cos\theta} \quad (1)$$

where:

k: shape factor, a constant depending on the crystal structure of the analyzed material. For magnetite (cubic crystals) and peak with Miller indexes (3 1 1), k = 0.9082

λ: wavelength of the X-ray source

β: line broadening at half the maximum intensity, after subtracting the instrumental line broadening, in radians

Θ: Bragg angle

Magnetic measurements were performed using a vibrating sample magnetometer (VSM Oxford, 3001) up to an applied field of 1.6 T. Hysteresis loops were measured at room temperature with a field scan rate of 5 Oe/s. TGA experiments were recorded from room temperature to 700°C in a High Resolution TGA Q5000 IR at a heating rate of 10°C/min in the presence of a continuous N_2 flow. The concentration of Cu^{2+} in all the samples was measured using a Shimadzu, AAS 6800 equipment.

Transmission electron microscopy (TEM) was performed using a JEM 2010-JEOL, operated at 120 kV. The x-ray photoelectron spectroscopy (XPS) study was carried out using an spectrometer XPS110 ThermoFisher-VG Instrument with a AlKα source (1486.7eV) at a base pressure better than 5×10^{-10} Torr. To correct the shifts in binding energies of core levels, the C-1s peak at 284.7 eV was used as an internal reference.

RESULTS AND DISCUSSION

Material Characterization

Figure 1 shows the FTIR spectrum of M1 as a representative sample (M2 exhibits similar spectrum). The intense band at 570 cm^{-1} corresponds to the valence vibration of Fe-O bonds in the Fe_3O_4 crystalline lattice (Babu and Dhamodharan 2008; Diamandescu et al. 2011). Such intense band is characteristic of ferrites with spinel or perovskites structure, due to the contribution in this region of vibrational bands related to the metal in the tetrahedral and octahedral sites of the oxide structure (Giraldo, Erto, and Pirajan 2013). The bands at 3346 cm^{-1}

and 1614 cm^{-1} have been attributed to vibrations of adsorbed water indicating the presence of moisture (Li et al. 2003; Liu et al. 2004).

Figure 2 shows the diffraction pattern for M1 sample, which is very similar to that of M2. The phase analysis of the diffractogram patterns showed that both samples are crystalline corresponding to an inverse spinel cubic structure of Fe_3O_4 or γ-Fe_2O_3. The presence of hematite (α-Fe_2O_3) on samples was excluded due to the absence of its more intense peaks occurring at 2θ = 38.814; 63.913 and 58.299 with hkl (104), (116) and (024) respectively, in accordance to the Powder Diffraction File 89-8104. The presence or absence of γ-Fe_2O_3 cannot be confirmed by this technique, because the reflections of the crystalline phase are very similar to those of Fe_3O_4 (Powder Diffraction File 89-0950 and 89-5894 respectively).

Average crystallite sizes were calculated according to the diffractograms and Scherrer quation using the most intense reflection at $2\theta = 41°$. Similar values were obtained for M1 (7.7 nm) and M2 (7.6 nm). The nanometer size of the samples was also evident in the magnetic measurements performed by VSM at room temperature. **Figure 3** displays the hysteresis loop corresponding to M2 sample, which achieves a saturation magnetization of 57.25 emu/g. The insert (-5 kOe < H < + 5 kOe) shows that the values of magnetic remanence (1.35 emu/g) and coercive field (10 Oe) are close to zero in correspondence with the superparamagnetic character of this sample. The magnetic measurement for M1 exhibits similar behavior. **Table 1** resumes the magnetic properties of both samples.

The difference between the Ms value and the massive Fe_3O_4 (90 emu/g) (Liu, Kaminski, Chen, et al. 2007; Liu, Kaminski, Riffle, et al. 2007) for all the samples, may be due to the nanometer size of the particles (Khan, Khattak, and Rahman 2011), the presence of impurities

and the oxidation of the sample during synthesis. Either the superparamagnetic character of samples or the average crystallite diameters determined by the Scherrer equation, supports the first hypothesis. The presence of impurities in the samples was confirmed in the FTIR discussed above, where it was noted that all the samples contained adsorption water. No evidence of oxidation was observed, but it is not excluded.

It is known that the value of Ms depends on the mass, hence by measuring the sample as a whole, it is necessary to take into account that the presence of non-magnetic impurities provokes the underestimation of Ms values (the impurities do not display magnetic response). In order to determine the percentage of impurities in each sample and to correct the Ms values, TGA data were recorded in the temperature range of 25-700°C under N_2 atmosphere. Two weight losses at 120°C and 350°C were found in both samples with global values of 8.14 wt% and 7.74 wt% for M1and M2, respectively. The weight loss at 120°C could be attributed to the removal of water (Morales 2007) and that at 350°C to the decomposition of an oxo-hydroxide (Prieto et al. 2009). The Ms values were corrected considering the total weight loss for each sample as shown in **Table 1**.

Figure 4 shows the TEM image and the distribution function using a log-normal fit. The nominal average diameter of the sample, obtained from an image analysis (Gatan Digital Micrograph 2.3.2) of the TEM micrograph, was $\langle D_{TEM} \rangle = 6.52 \pm 0.06$ nm and dispersion $\sigma = 0.27$. This result corroborates the diameter mean size calculated by Scherrer`s method linked to XDR measurements.

Influence of pH and Time of Interaction in Removal of Cu^{2+} from Solutions

Determination of the pH of Maximum Adsorption

Figure 5a shows the amounts of Cu^{2+} remaining in solution as a function of pH after being filtered from the adsorption experiments with Fe_3O_4 nanoparticles. As observed, the amount of Cu^{2+} in the solution decreases with increasing pH for P solution at pH > 4 and for M1 and M2 solutions at pH > 2.

The change of Cu^{2+} concentration with pH observed for P solution is due to the formation of $Cu(OH)_2$, which has a solubility product constant (Ksp) of $2.00x10^{-15}$ at 25°C. (Karami 2013) At the experimental conditions the precipitation of the hydroxide begins at pH > 4.

The decrease in the Cu^{2+} concentration for M_i solutions was more pronounced than for the P solution, indicating the occurrence of Cu^{2+} adsorption onto the Fe_3O_4 surface. This evidence can be clearly observed at pH values between 2 and 4 where the concentration of Cu^{2+} in the P solution is practically the same.

The decrease of Cu^{2+} concentration with increasing pH in M_i solutions is in agreement with previous reports (Hu, Chen, and Lo Masce 2006; Katsumata et al. 2003; Roy and Bhattacharya 2012; Giraldo, Erto, and Pirajan 2013; Karami 2013). The reasons attributed to this behavior are:

1) The formation of surface complexes ((SFeO)qCur(OH)s(2-qs)) according to:

$$SH_2O_{(ac)} + q\,SFeOH_{(s)} + rCu^{2+}{}_{(ac)} \rightleftharpoons (SFeO)_qCu_r(OH)_{s(s)}^{(2-q-s)} + (s+q)H^+(ac) \qquad (2)$$

where $(SFeO)_qCu_r(OH)_s^{(2-q-s)}$ is the complex formed on the surface of magnetite, where **s**, **q** and **r** are the stoichiometric coefficients. Increasing pH shifts the equilibrium to the formation of the surface complex, resulting in a greater adsorption of Cu^{2+} by the adsorbent (Giraldo, Erto, and Pirajan 2013).

2) The surface charge density of magnetite decreases with increasing pH. Different values of isoelectric point (IP) have been reported, for instance 7 (Vergés et al. 2008), 6.5 (Khalafalla and Reimers 1980) and 6 (Yanglong, Junfeng, and Song 2003). The surface charge density is positive for pH < PI and negative for pH > PI (Yanglong, Junfeng, and Song 2003), so that the increase of pH favors the adsorption of Cu^{2+} ions on the surface of magnetite by electrostatic attraction.

The adsorption of Cu^{2+} on the magnetite surface was observed by XPS measurements. **Figure 6** shows that the general survey scans of the samples of magnetite before and after the adsorption process are similar but around 930-950 eV the sample of magnetite after Cu^{2+} adsorption displays small anomalies associated to Cu-2p.

3) The formation of Cu(OH)2 with increasing pH, which was measured by means of blank solutions.

The amount of Cu^{2+} adsorbed on a sample of Fe_3O_4 nanoparticles at different pH values can be estimated by measuring either the content of Cu^{2+} in the solid or the amount of Cu^{2+} species remaining in the solution. The second choice is easier to achieve, but it requires to take into account the likely formation of insoluble $Cu(OH)_2$ in order to avoid incorrect results. For instance, Karami (2013) reported that a sample of magnetite can adsorb 76 mg/g of Cu^{2+} at pH = 5.5. This estimation was obtained by determining the Cu^{2+} remaining in solution, whose initial concentration was 10 mg/L, after a contact time of 60 mins. The author assumed that all the Cu^{2+} removed from the solution was captured by magnetite. However, the formation of $Cu(OH)_2$ is possible according to the initial content of Cu^{2+}, the pH value of the solution, and the value of Kps for $Cu(OH)_2$. Hence, the reported adsorption value (76 mg/g at pH = 5.5) is likely to be overestimated.

Analogous study was carried out by Giraldo (Giraldo, Erto, and Pirajan 2013) and Predescu (Predescu et al. 2012), who made the same assumption and reported, consequently, overestimated values of Cu^{2+} adsorption. Giraldo also considered that the formation of $Cu(OH)_2$ prevents the determination of the adsorption capacity of magnetite toward Cu^{2+} ions at high pH values. Albeit, our results support that using a blank (the P solutions) allows a good estimation of the adsorption capacity at pH values as high as 9.

In fact, **Figure 5b** shows the amounts of Cu^{2+} adsorbed by Fe_3O_4 samples at pH values between 2 and 9. These data were calculated by subtracting the mass of Cu^{2+} ions obtained in P solution, from those of the M_i solutions at each pH value. The resulting adsorption data present a maximum at pH = 7. This procedure ensures that the observed decrease of Cu^{2+} content in the solution is only due to the effective adsorption by Fe_3O_4 sample.

Kinetics of the Adsorption of Cu^{2+} Ions by Magnetite

The uptake of Cu^{2+} ions by magnetite samples, M1 and M2, at pH 7.0, shaking rate of 120 rpm and at 30 ^{o}C, increases with time. At t = 445 and 490 mins for M1 and M2 respectively the adsorption of Cu^{2+} reaches a maximum value that does not change appreciably at longer times ($\Delta q < 0.001$ mg/g). This behavior is illustrated in **Figure 7**. All curves indicate an increasing trend of the adsorption of Cu^{2+} to a constant value, in agreement with previous studies (Hu, Chen, and Lo Masce 2006; Predescu et al. 2012; Giraldo, Erto, and Pirajan 2013; Karami 2013). The plateau corresponds to the maximum adsorption or the equilibrium amount of adsorbed Cu^{2+} ions (q_{eq}). The initial time of the plateau was considered as the minimum time (t_{min}) to reach the maximum adsorption as indicated in **Figure 7**.

Due to the Cu^{2+} adsorption is expressed in mg of Cu^{2+}/g of Fe_3O_4 the maximum adsorption and the adsorption capacity of magnetite coincide. These values, as well as the removal percentages are summarized in **Table 2**. The adsorption equilibrium of M1 and M2 is reached at 445 and 490 mins by showing an adsorption capacity of 3.11 and 6.28 mg/g respectively.

The characterization of samples M1 and M2 showed not differences between them except Ms value which is larger for the second sample ($Ms_{M2} = 1.2Ms_{M1}$) and is likely to be responsible of the higher adsorption capacity found for M2.

The data of **q** versus **t** can be linearized helping to explain the adsorption mechanism. Basically, two models are considered as a liquid/solid phase reaction, pseudo-first and pseudo-second order reaction (Roy and Bhattacharya 2012).

According to the adsorption rate (dq/dt):

$$\frac{dq}{dt} = k(q_{eq} - q)^n \qquad (3)$$

The integrated equation for n = 1 is:

$$ln\left(q_{eq} - q\right) = -k_1 t + lnq_{eq} \qquad (4)$$

and for n = 2, after integration and rearrangement:

$$\frac{t}{q} = \frac{1}{h} + \frac{1}{q_{eq}} t \quad (5)$$

Where:

$$h = k_2 q_{eq}^2 \qquad (6)$$

The pseudo-first order model is associated with either film diffusion or intra-particle diffusion; while the pseudo-second order model is related to chemical adsorption.

The experimental data deviate considerably from the pseudo-first order model, but match very well with the pseudo-second order model. **Figure 8** shows the linear plots of t/q against t with correlation coefficients greater than 0.99 for both curves. Values of q_{eq} were calculated from the slop and intercept of the straight lines according to equation 5 and the results are shown in **Table 3**. These values are practically equal to those reported in **Table 2**.

The kinetic behavior suggests that the sorption system Cu^{2+}-magnetite is consistent with the pseudo-second order model; hence, we can affirm that the rate-limiting step comprises chemisorption processes.

CONCLUSION

The co-precipitation method of salts yielded magnetite nanoparticles with saturation magnetization values of 52 (M1) and 62 (M2) emu/g. The maximum adsorption of Cu^{2+} ions by the synthesized Fe_3O_4 nanoparticles occurs at pH = 7. Sample M2 adsorbs more Cu^{2+} than sample M1 and the adsorption equilibrium is reached at a similar time. The use of blank solutions avoids overestimation of the adsorption capacity due to the presence of insoluble $Cu(OH)_2$ at pH > 4. The adsorption kinetics is well described by a pseudo-second order model, which suggests that the main adsorption mechanism comprise chemisorption.

Acknowledgements

We want to thank the technic staff from the University Laboratory of Characterization of Substance Structure (LUCES), at the Institute of Material Science and Technology (IMRE),

Cuba, for providing facilities and equipment for carrying out this work. We also want to thank to Ing. Martin Hernandez Landaverde, from the Queretaro Unit of CINVESTAV-IPN (Mexico) for performing X-ray diffractograms and Dr. Edilso Reguera of IMRE from CICATA-Legaria, IPN (México), for TGA measurements. We thank Dr. Fabienne Barroso Bujans for her valuable criticism.

References

Babu, K., and R. Dhamodharan. 2008. Grafting of poly(methyl methacrylate) brushes from magnetite nanoparticles using a phosphonic acid based initiator by ambient temperature atom transfer radical polymerization (ATATRP). *Nanoscale Research Letters* 3:109–17. doi:10.1007/s11671-008-9121-9

Chen, K., Y. Zhu, Y. Zhang, L. Li, Y. Lu, and X. Guo. 2011. Synthesis of magnetic spherical polyelectrolyte brushes. *Macromolecules* 44:632–39. doi:10.1021/ma102337c

Cotten, G. B., J. D. Navratil, and H. B. Eldredge. 1999. Magnetic adsorption method for the treatment of metal contaminated aqueous waste. WM'99 Conference.

Davidson, J. 2010. *Removal of nickel(II) from aqueous solutions by polymer-enhanced ultrafiltration*. Worcester Polytechnic Institute, Environmental Science and Engineering, Shanghai Jiao Tong.

Diamandescu, L., F. Tuna, T. Popescu, D. Gingasu, I. Mindru, L. A. Patron, and J. M. Calderon-Moreno. 2011. Investigation of magnetiteformation in the presence of hidrazine dihidrochloride digest. *Journal of Nanomaterials and Biostructures* 6 (3):1065–72.

Farrukh, A., A. Akram, A. Ghaffar, S. Hanif, A. Hamid, H. Duran, and B. Yameen. 2013. Design of polymer-brush-grafted magnetic nanoparticles for highly efficient water remediation. *ACS Applied Materials & Interfaces* 5: 3784–93. doi:10.1021/am400427n

Fu, F., and Q. Wang. 2011. Removal of heavy metal ions from wastewaters: A review. *Journal of Environmental Management* 92:407–18.

Giraldo, L., A. Erto, and J. C. M. Pirajan. 2013. Magnetite nanoparticles for removal of heavy metals from aqueous solutions: Synthesis and characterization. *Adsorption* 19:465–74. doi:10.1007/s10450-012-9468-1

Gong, T., D. Yang, J. Hu, W. Yang, C. Wang, and J. Q. Lu. 2009. Preparation of monodispersed hybrid nanospheres with high magnetite content from uniform Fe3O4 clusters. *Colloids and Surfaces A: Physicochemical and Engineering Aspects* 339:232–39. doi:10.1016/j.colsurfa.2009.02.034

Hu, J., G. Chen, and I. M. C. Lo Masce. 2006. Selective removal of heavy metals from industrial wastewater using maghemite nanoparticle: Performance and mechanisms. *Journal of Environmental Engineering* 132 (7):709–15. doi:10.1061/(asce)0733-9372(2006)132:7(709)

Jiuhui, Q. U. 2008. Research progress of novel adsorption processes in water purification: A review. *Journal of Environmental Sciences* 20:1–13. doi:10.1016/s1001-0742(08)60001-7

Karami, H. 2013. Heavy metal removal from water by magnetite nanorods. *Chemical Engineering Journal* 219:209–16. doi:10.1016/j.cej.2013.01.022

Katsumata, H., S. Kaneco, K. Inomata, K. Itoh, K. Funasaka, K. Masuyama, T. Suzuki, and K. Ohta. 2003. Removal of heavy metals in rinsing wastewater from plating factory by adsorption with economical viable materials. *Journal of Environmental Management* 69:187–91. doi:10.1016/s0301-4797(03)00145-2

Khalafalla, S. E., and G. W. Reimers. 1980. Preparation of dilution-stable aqueous magnetic fluids. *IEEE Transactions on Magnetics* 16 (2):178–83. doi:10.1109/tmag.1980.1060578

Khan, U. S., N. S. Khattak, and A. Rahman. 2011. Historical development of magnetite nanoparticles synthesis. *Journal of the Chemical Society of Pakistan* 33 (6):793–804.

Li, T., Y. Deng, X. Song, Z. Jin, and Y. Zhang. 2003. The formation of magnetite nanoparticle in ordered system of the soybean lecithin. *Bulletin of the Korean Chemical Society* 24 (7):957–60. doi:10.5012/bkcs.2003.24.7.957

Liu, X., Q. Hu, Z. Fang, X. Zhang, and B. Zhang. 2009. Magnetic chitosan nanocomposites: A useful recyclable tool for heavy metal ion removal. *Langmuir* 25:3–8. doi:10.1021/la802754t

Liu, X., M. D. Kaminski, H. Chen, and M. Torno. 2007. Synthesis and characterization of highly-magnetic biodegradable poly(D,L-lactide-co-glycolide) nanospheres. *Journal of Controlled Release* 119:52–58.

Liu, X., M. D. Kaminski, J. S. Riffle, H. Chen, M. Torno, M. R. Finck, L. Taylor, and A. J. Rosengart. 2007. Preparation and characterization of biodegradable magnetic carriers by single emulsion-solvent evaporation. *Journal of Magnetism and Magnetic Materials* 311:84–87. doi:10.1016/j.jmmm.2006.10.1170

Liu, Z. L., X. Wang, K. L. Yao, G. H. Du, Q. H. Lu, Z. H. Ding, J. Tao, Q. Ning, X. P. Luo, D. Y. Tian, and D. Xi. 2004. Synthesis of magnetite nanoparticles in W/O microemulsion. *Journal of Materials Science* 39:2633–36.

Massart, R. 1981. Preparation of aqueous magnetic liquids in alkaline and acidic media. *IEEE Transactions on Magnetics* 17 (2):1247–48. doi:10.1109/tmag.1981.1061188

Morales, J. P. U. 2007. *Síntesis de Nanopartículas Magnéticas y su Implementación como Ferrofluidos*. Medellín: Ciencias Exactas y Naturales, Universidad de Antioquia.

Navratil, J. D., and A. C. Akin. 2009. Mine water treatment using magnetite and iron ferrites. Paper read at International Mine Water Conference, South Africa.

Ortiz, N. 2000. ESTUDO DA UTILIZAÇÃO DE MAGNETITA COMO MATERIAL ADSORVEDOR DOS METAIS Cu 2, Pb 2, Ni 2 E Cd 2, EM SOLUÇÃO, Universidade de São Paulo.

Predescu, A., E. Matei, A. Predescu, and A. Berbecaru. 2012. Removal efficiency on magnetite (Fe_3O_4) of some multicomponent systems present in synthetic aqueous solutions. Paper read at Recent Researches in Communications, Electronics, Signal Processing and Automatic Control.

Prieto, N., M. Castro, R. Morales, M. Herrera, R. Mata, and M. Carreón. 2009. Caracterización de la Sinterización de Pelets Elaborados de Mezclas de Mineral de Hierro Magnetita-Hematita. In *Foro de Ingeniería e Investigación en Materiales*, ed. E. A. Aguilar, J. Lemus, E. Bedolla, and C. A. León. Morelia, México.

Roy, A., and J. Bhattacharya. 2012. Removal of Cu(II), Zn(II) and Pb(II) from water using microwave-assisted synthesized maghemite nanotubes. *Chemical Engineering Journal* 211–12:493–500. doi:10.1016/j.cej.2012.09.097

Soltero-Baeza, D., D. S. Palafox-González, I. R. Herrera-Baeza, A. Dávila-Sánchez, J. M. Cuéllar-Miramontes, and M. O. González-Rangel. 2007. Determinación de Niveles de Cobre en una Población Estudiantil por Espectrofotometría de Absorción Atómica en Flama. *Aventuras del Pensamiento* 1–6.

Teja, A. S., and P.-Y. Koh. 2009. Synthesis, properties, and applications of magnetic iron oxide nanoparticles. *Progress in Crystal Growth and Characterization of Materials* 55:22–45. doi:10.1016/j.pcrysgrow.2008.08.003

Vergés, M. A., R. Costo, A. G. Roca, J. F. Marco, G. F. Goya, C. J. Serna, and M. P. Morales. 2008. Uniform and water stable magnetite nanoparticles with diameters around the monodomain–multidomain limit. *Journal of Physics D: Applied Physics* 41 (13):134003. doi:10.1088/0022-3727/41/13/134003

Yanglong, H., Y. Junfeng, and G. Song. 2003. Solvothermal reduction synthesis and characterization of superparamagnetic magnetite nanoparticles. *Journal of Materials Chemistry* 13:1983–87.

Table 1. Magnetic properties measured for Fe_3O_4 samples

Sample	Ms (emu/g)	Ms corrected (emu/g)	Mr (emu/g)	Hc (Oe)
M1	47.25	51.75	0.79	12
M2	57.00	61.89	1.35	10

Table 2. Minimum time of maximum adsorption (t_{min}) and maximum capacity of Cu^{2+} ion extracted per gram of magnetite (capture capacity)

Adsorbent characteristics	Sample M1	Sample M2
Removal percentage	86	96
t_{min} (min)	445 ± 10	460 ± 20
Capture capacity (mg/g)	3.11 ± 0.06	6.26 ± 0.09

Table 3. Kinetics parameters for Cu^{2+} ions adsorption by magnetite according to the pseudo-second order model[1]

Magnetite	H (mg/(g × min)	k_2 (g/(mg × min)	q_{eq} (mg/g)	R^2
M1	0.4 ± 0.3	0.04 ± 0.05	3.156 ± 0.001	0.9996
M2	0.4 ± 0.4	0.01 ± 0.02	6.254 ± 0.001	0.9983

[1] $\frac{t}{q} = \frac{1}{h} + \frac{1}{q_{eq}} t$ and $h = k_2 q_{eq}^2$.

Figure 1. Fourier transformer infrared spectrum (FTIR) of magnetite sample M1.

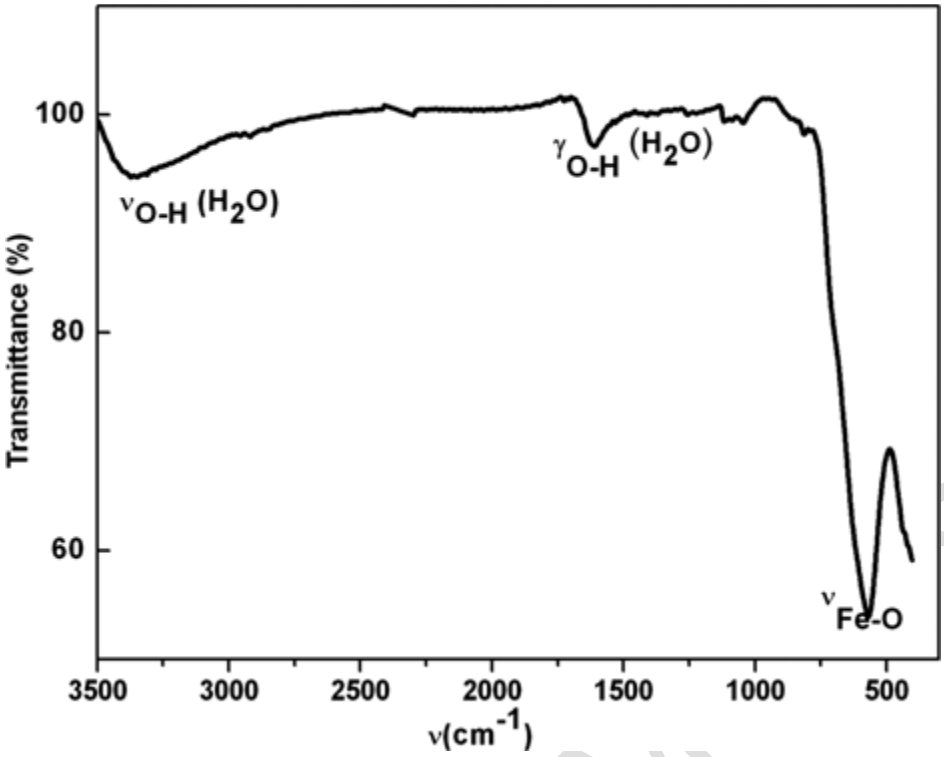

Figure 2. Diffraction pattern with Kα-Co radiation of magnetite sample M1.

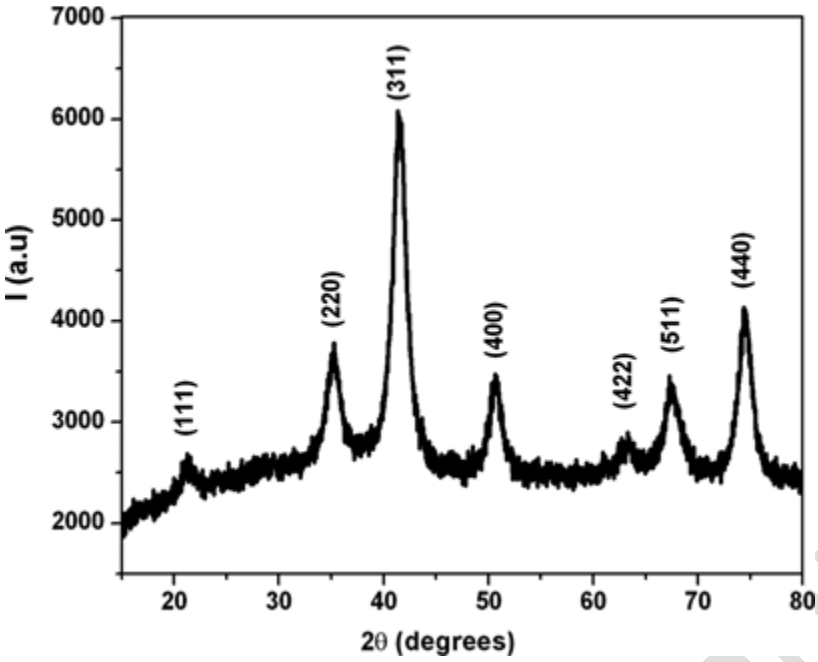

Figure 3. Hysteresis loop at room temperature of magnetite sample M2. Insert shows the hysteresis loop in the region –5kOe < H < + 5 kOe, field speed 5 Oe/s.

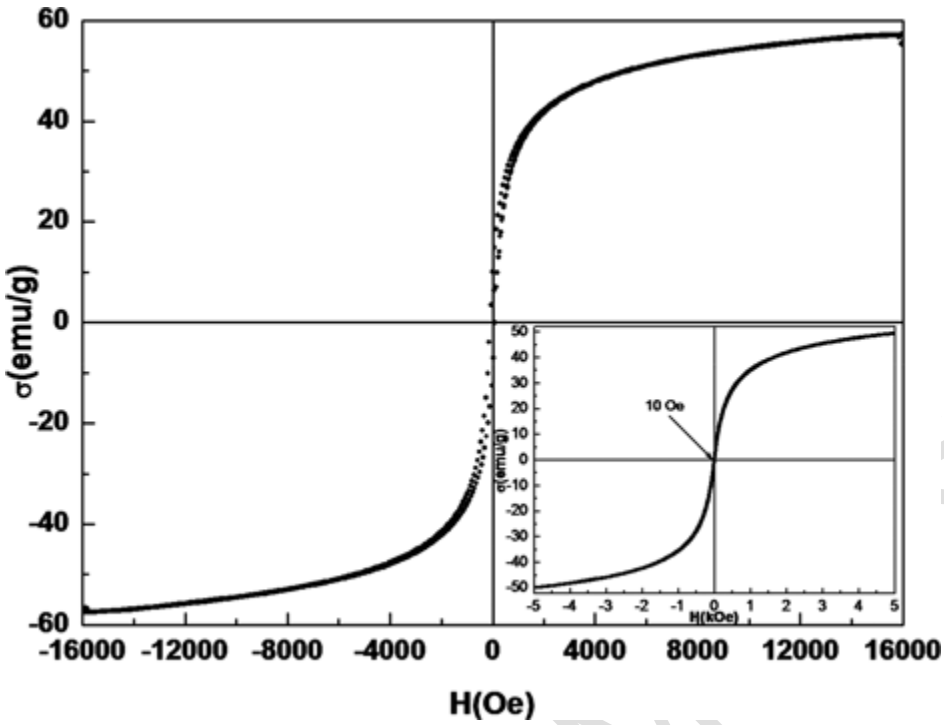

Figure 4. (a) TEM image of magnetite sample M1. (b) Distribution function of nanoparticles and log-normal fit.

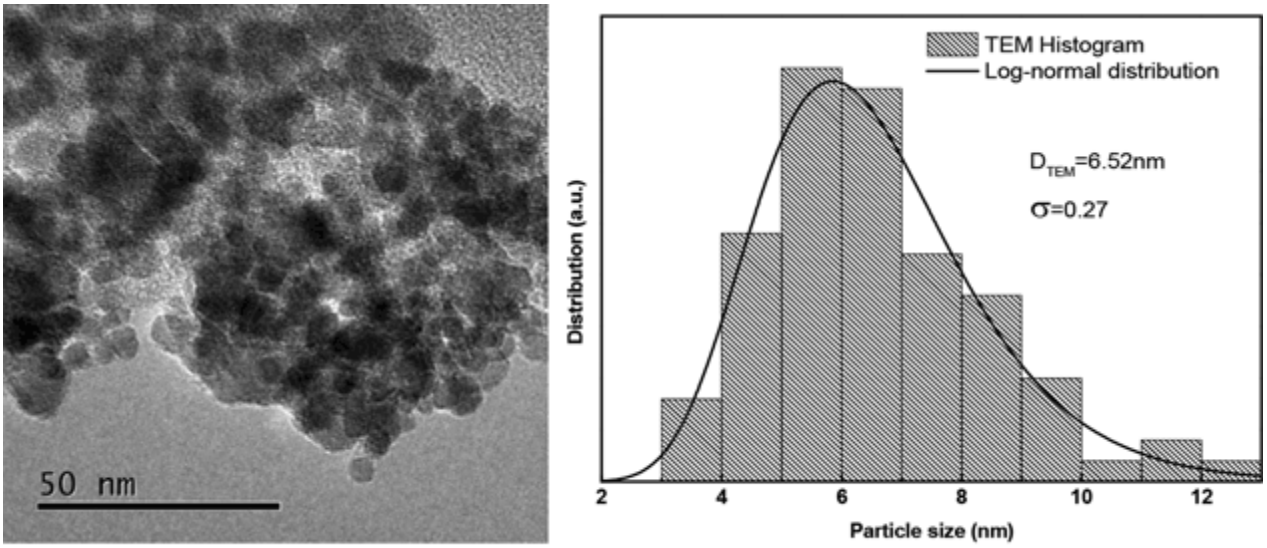

(a) (b)

Figure 5. (a) pH effect on the amount of Cu^{2+} ions remaining in the blank, M1 and M2 solutions. (b) Effect of pH on the Cu^{2+} mass adsorbed by magnetite.

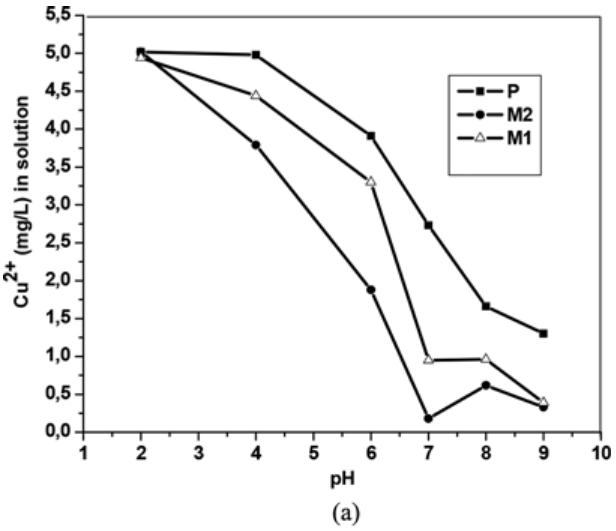

(a)

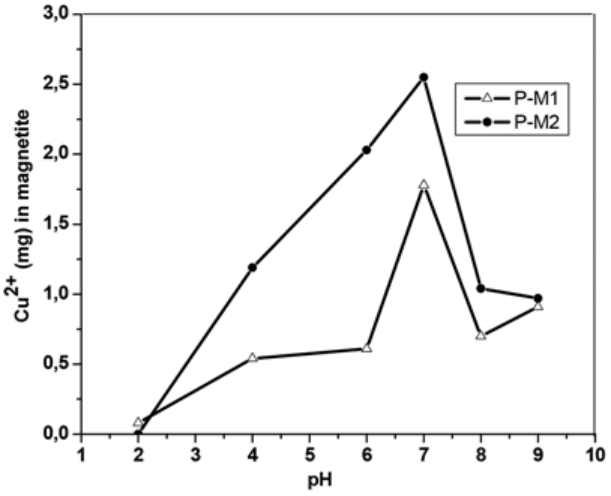

(b)

Figure 6. XPS spectroscopy survey scans of nanoparticles before (pure Fe_3O_4) and after the Cu adsorption respectively. The inset shows, the high resolution peaks for copper doublet Cu at 933.52 and 953.32 eV which corresponding to Cu $2p_{3/2}$ and Cu $2p_{1/2}$ spin-orbit splitting, respectively.

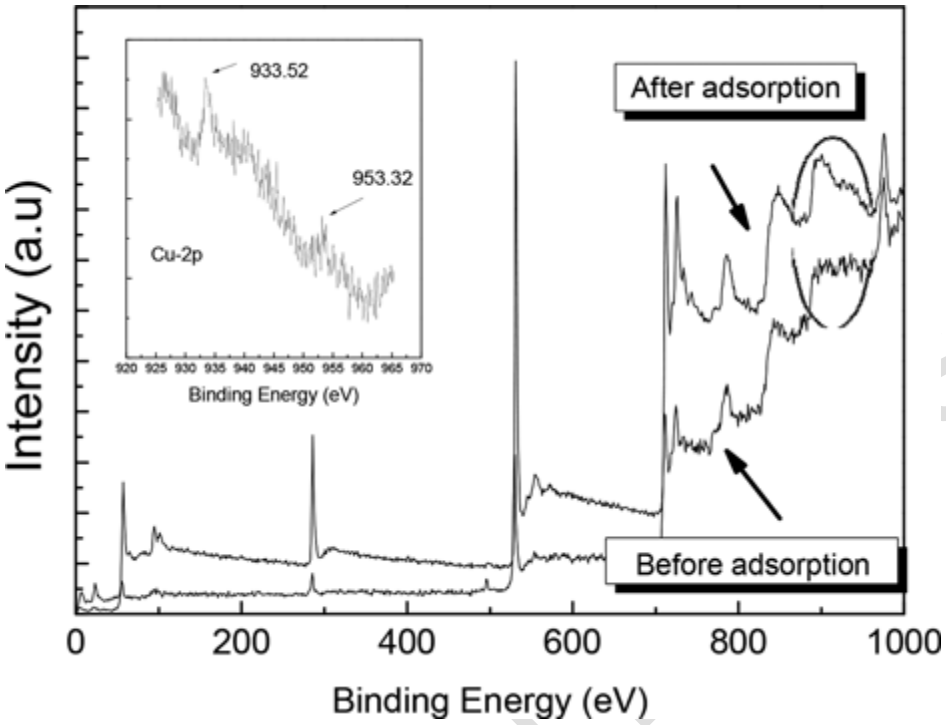

Figure 7. Effect of contact time on the uptake of Cu2+ ions by magnetite samples M1 and M2, $[Cu(NO_3)_2]_o$ = 10 mg/L, [magnetite] = 102 mg/L, pH = 7.0, shaking rate: 120 rpm, T = 30°C). Arrows indicate the t_{min} and the maximum adsorption values.

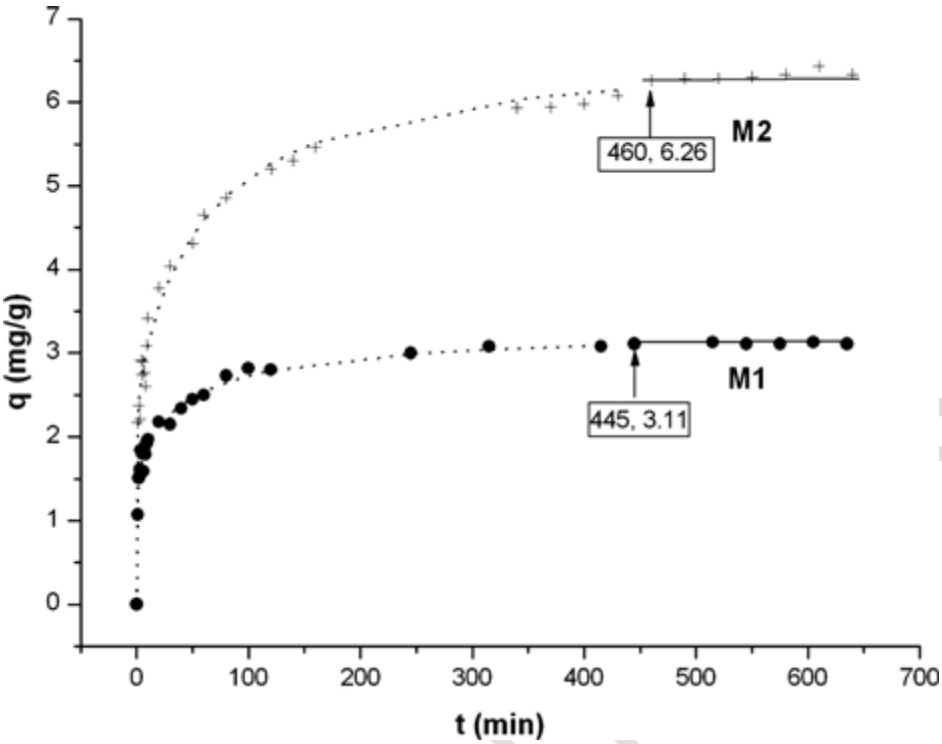

Figure 8. Kinetic curves of pseudo-second order corresponding to the adsorption of Cu^{2+} ions by magnetite samples (M1 and M2) at pH = 7 and T = 30°C.